X-ray crystallographic structure of a papain–leupeptin complex

Ewald Schröder, Christopher Phillips, Elspeth Garman, Karl Harlos and Catherine Crawford

University of Oxford, Laboratory of Molecular Biophysics, The Rex Richards Building, South Parks Road, Oxford, OX1 3QU, UK.

The three-dimensional structure of the papain–leupeptin complex has been determined by X-ray crystallography to a resolution of 2.1 Å (overall R-factor = 19.8%). The structure indicates that: (i) leupeptin contacts the S subsites of the papain active site and not the S′ subsites; (ii) the 'carbonyl' carbon atom of the inhibitor is covalently bound by the Cys-25 sulphur atom of papain and is tetrahedrally coordinated; (iii) the 'carbonyl' oxygen atom of the inhibitor faces the oxyanion hole and makes hydrogen bond contacts with Gln-19 and Cys-25.

1. INTRODUCTION

Properties of the plant protease papain have been widely investigated since it is a typical example from the cysteine protease family. A variety of low molecular weight inhibitors of papain have been described [1–4]. Three dimensional structures have been reported for papain complexed with chloromethyl ketones [5], E-64 [1-[*N*-[(L-3-*trans*-carboxyoxirane-2-carbonyl)-L-leucyl]-amino]-4-guanidinobutane] [6] and E-64c [(+)-(2*S*, 3*S*)-3-(1-[*N*-(3-methylbutyl)amino]leucylcarbonyl)oxirane 2-carboxylic acid] [7–8].

Papain is also inhibited by the peptide aldehyde leupeptin (Ac-Leu-Leu-Arginal) (Fig. 1) [9]. Leupeptin has broad specificity; it inhibits other cysteine proteases [4] as well as certain serine proteases (for example plasmin and trypsin). Leupeptin has been used to investigate the possible role of proteases in tumour cell invasion and metastasis [10], protein synthesis [11] and muscular dystrophy [12].

Leupeptin binds reversibly to papain. The reaction occurs in two steps [4].

$$E + I \rightleftharpoons E\,I \rightleftharpoons E\,I'$$
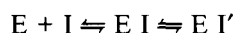
The inhibitor **I** binds non-covalently to the active site of the enzyme **E** and forms the Michaelis complex **EI**. In the second step the active-site nucleophile of the protease attacks the aldehyde carbon atom of the bound inhibitor to form a hemithioacetal structure **EI′**. This complex represents a transition state analogue. It is tight binding with a $K_d = 10^{-9}$ M for the binding of leupeptin to papain [13]. In solution leupeptin exists as an equilibrium between three species: cyclic hemiami-

nal, free aldehyde and hydrated aldehyde, of which only the free aldehyde (2%) can inhibit protease activity [13].

Although peptide aldehydes have been well studied and are useful inhibitors of cysteine proteases, no three-dimensional structures of aldehyde–cysteine protease complexes have been reported to date. The X-ray crystallographic structure of such a complex between leupeptin and papain is described here.

2. EXPERIMENTAL

Crystals of the papain–leupeptin complex were grown at 4°C in 5–10 days by the sitting drop method. The reservoir contained 500 μl of H$_2$O /methanol (1:2) and 60 μl of saturated NaCl, while the sitting drop contained 30 μl of inhibited papain. Crystals of the complex were dissolved and assayed for caseinolytic activity in the presence of methanol (67%) and leupeptin [15]. The results confirmed that the activity of the crystals was 100% inhibited when compared with native papain assayed in the presence of methanol.

X-ray diffraction data were collected from the crystals on a Siemens

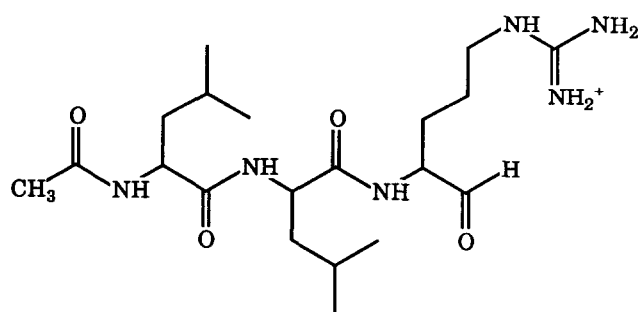*Correspondence address:* C. Crawford, University of Oxford, Laboratory of Molecular Biophysics, The Rex Richards Building, South Parks Road, Oxford, OX1 3QU, UK. Fax: (44) (865) 510454.

Fig. 1. Chemical structure of leupeptin (taken from [12])

area detector with monochromated Cu-Kα X-ray radiation. The crystals were orthorhombic and belonged to space group $P2_12_12_1$. The unit cell parameters were : $a = 44.92$ Å, $b = 104.96$ Å, $c = 50.97$ Å. The crystals were isomorphous with the 1.65 Å papain structure present in the Brookhaven data bank (reference 9pap) [16]. The diffraction data gave a total of 12452 unique reflections to 2.1 Å (88% complete) of which 11026 had $F_o \geq 2\sigma$ (F). The merging R-factor for the intensities over all data was 9.4%. The structure factors were phased using the atomic coordinates of native papain. A model of papain was fitted into the electron density and had an unrefined R-factor of 34.4%. The model was refined using the XPLOR package [17]. A $(2F_o-F_c)$ exp$^{i\alpha c}$ difference map was calculated and showed the presence of a 'tube' of electron density lying within the active site groove (Fig. 2).

A model of the leupeptin molecule was fitted into the electron density using FRODO [18] on an Evans and Sutherland ESV-10 graphics workstation and refined. The difference map clearly indicated that the 'carbonyl' oxygen atom of the molecule was facing into the 'oxyanion hole' [4] (Fig. 3). The 'carbonyl' carbon atom was tetrahedral (angles set to 109.5° with force constants 45–50 kcal/mol·rad^{-2}) and covalently bound to the sulphur atom of Cys-25 (bond length set to 1.81 Å).

A total of 211 bound solvent molecules (water and methanol) were added to the model structure. The solvent molecules in the vicinity of

the active site were refitted. The complex was then further refined over all data between 20 Å and 2.1 Å and a correction for the bulk solvent scattering was included. The final model has a residual of 19.8% over all data (Fig. 4).

3. RESULTS

The refined model indicates that the inhibitor molecule is bound within the active site by a combination of hydrogen bonds and hydrophobic interactions (Table I, Fig. 4).

The rms deviation for all bond lengths from ideal stereochemistry was 0.013 Å, while the angles exhibited an rms deviation of 2.33°. The structure showed that the aldehyde had reacted to form a tetrahedral hemithioacetal, with the oxygen atom facing the papain oxyanion hole. Leupeptin reacted stereospecifically, giving an 'S' stereoisomer [19]. The angles about the asymmetric 'carbonyl' carbon atom in the refined structure fell within the range 91.3° to 117°. The sulphur–carbon bond length refined to 1.65 Å, which is shorter than the 1.81 Å imposed as the restraint. The distance between the Nδ1 atom of His-159 and the sulphur atom of Cys-25 is 3.79 Å, compared to 3.65 Å in the native structure. The proton attached to the 'carbonyl' carbon atom is in the same plane as the imadazolium group of His-159. The imadazolium is therefore in the correct orientation for the Nδ1 atom to donate a proton to a potential leaving group [5].

The papain subsites contacted are the S subsites as opposed to the S' subsites [20] and this is consistent with the binding observed in the crystal structures of papain with other inhibitors [5–8,21]. The S$_2$ subsite within the papain active site has been identified as the hydrophobic pocket enclosed by the side-chains of Tyr-67, Pro-68, Phe-207, Val-133 and Val-157. The leucyl group at position P$_2$ of the inhibitor is observed to bind within the S$_2$ subsite while the leucyl group at position P$_3$ is likely to be involved in hydrophobic interactions with Tyr-61 and Tyr-67 at the edge of the pocket. The backbone of the leucine at the P$_2$ position of the inhibitor forms a one residue stretch of antiparallel β-sheet with Gly-66. The arginine side chain at the P$_1$ position makes hydrogen bonds with three waters and with one methanol molecule. Two of the same water molecules mediate indirect hydrogen bonds between the 4-guanidinobutane head group of the arginine side-chain and the backbone carbonyl groups of Val-157 and Asn-64. In addition it is likely that the methyl groups of two methanols form hydrophobic contacts with the arginine side-chain at the Cβ and Cγ positions.

Comparison of the enzyme structure in the leupeptin complex with the native papain structure indicated that the binding of leupeptin has induced only minor adjustments in the conformation of the active site. The ring structure of Tyr-61 has twisted away from the inhibitor presumably in order to accommodate the leucyl group

Fig. 2 A $(2F_o-F_c)$ exp$^{i\alpha c}$ difference map (contoured at 0.260 e/Å^3) calculated for the initial, partly refined model (R=26%), as seen from 'within' the active site cleft. This model did not assume the presence of an inhibitor molecule bound to the papain. The positions of the Cys-25 sulphur atom and of the His-159 and Tyr-67 residues are indicated with respect to the difference electron density.
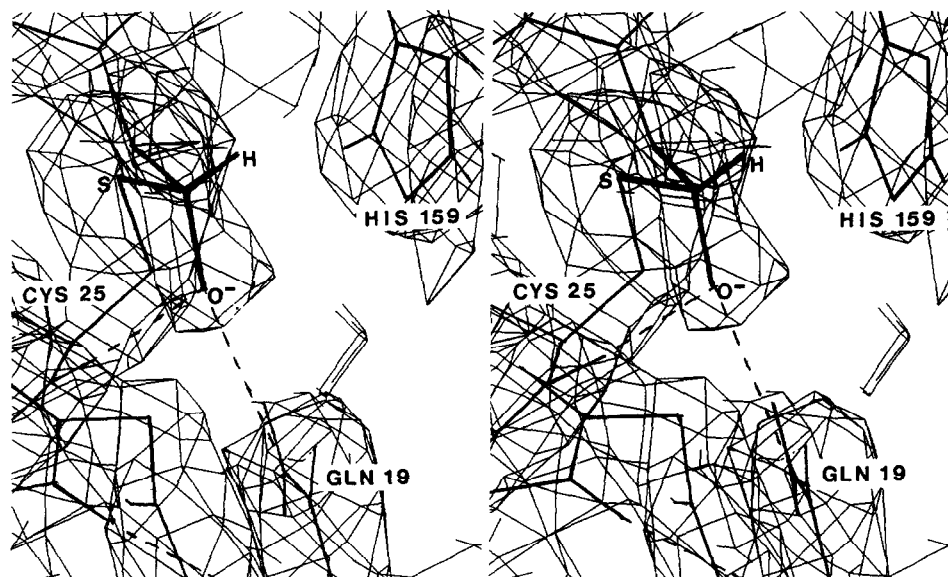
Fig. 3. A stereopair showing the $(2F_o-F_c)\exp^{i\alpha_c}$ difference map (contoured at 0.300 e/$\mathring{A}^3$) calculated from the fully refined model and highlighting the tetrahedral coordination centred upon the asymmetric carbon atom. The leupeptin molecule is indicated in heavy outline with respect to the papain active site. The dotted lines indicate hydrogen bonds (less than 3.5 $\mathring{A}$).

at the P_3 position of the inhibitor. The C-Cα bond has rotated by 11°, the Cα-Cβ bond by 23° and the Cβ-Cγ bond by 41°. At the opposite end of the active site cleft, the Cβ-Cγ bond of the Asn-64 residue has rotated by 24°.

4. DISCUSSION

A variety of intermediates are generated when papain reacts with substrate or an inhibitor, and the reaction pathway has been widely described [22–26] and re-
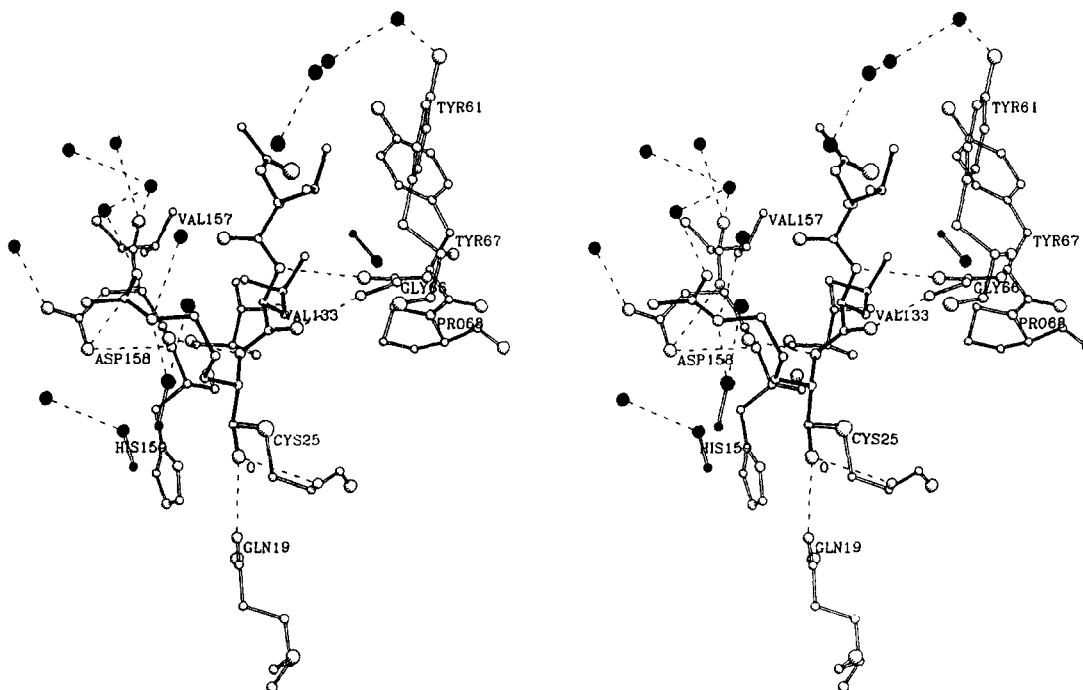

Fig. 4. Stereopair showing the leupeptin molecule bound within the papain active site. The inhibitor is shaded dark and the papain residues it contacts are indicated. Bound waters are represented as filled spheres and bound methanols as filled 'dumb-bells'. Hydrogen bonds are represented as dashed lines. The view is looking into the active site.

Table I

Summary of the papain-leupeptin interactions. See text for a description of the interactions with the bound solvent molecules

Type of Interaction	Leupeptin residue	Leupeptin atom	Papain residue contacted	Papain atom contacted	Bond Length (Å)
Hydrogen bonds (< 3.5 Å)	P1 (Arg)	Oxyanion	Gln-19	Amide nitrogen of sidechain	2.9
	P1 (Arg)	Oxyanion	Cys-25	Amide nitrogen of backbone	3.0
	P1 (Arg)	Amide nitrogen of backbone	Asp-158	Carbonyl oxygen of backbone	2.9
	P2 (Leu)	Carbonyl oxygen of backbone	Gly-66	Amide nitrogen of backbone	2.9
	P2 (Leu)	Amide nitrogen of backbone	Gly-66	Carbonyl oxygen of backbone	3.1
Hydrophobic contacts (3.5–5.0 Å)	P2 (Leu)		Tyr-67		> 4.5
	P2 (Leu)		Pro-68		> 3.9
	P2 (Leu)		Val-133		> 3.8
	P2 (Leu)		Val-157		> 4.7
	P3 (Leu)		Tyr-61		> 3.8
	P3 (Leu)		Tyr-67		> 3.6

viewed [3,27]. The reaction of papain with an aldehyde inhibitor has long been assumed to generate a 'dead-end' tetrahedral structure, analogous to the transient thiolester transition state observed during the catalysis of substrate by papain. Bendall et al. [25] using ^{1}H NMR were the first to provide evidence for the presence of a proton attached to a tetrahedral carbon atom. Evidence for a tetrahedral complex was also given by Mackenzie et al. [19] who applied ^{13}C NMR spectroscopy to papain complexed with N-acetyl-D- and N-acetyl-L-phenylalanyl[1-^{13}C]glycinal. There has been some controversy concerning the orientation of the atoms in the tetrahedral complex, specifically, whether or not the oxygen is facing the oxyanion hole. Mackenzie et al. [19] postulated from their ^{13}C NMR data that the oxygen atom pointed away from the oxyanion hole. Menard et al. [22] have suggested that stabilisation of the oxygen atom by Gln-19 in the oxyanion hole is important in the catalysis of substrates, but not in the reaction of papain with an aldehyde inhibitor. Others have suggested that stabilisation of the transition state by the oxyanion hole is not even essential for the hydrolysis of substrate by papain [28–29] (reviewed in [3,27]). Drenth has constructed a model for a tetrahedral intermediate by modifying the structure derived from papain inhibited with chloromethyl ketone [5]. In contrast to the data discussed above, this adduct showed the oxygen atom to be stabilized in the oxyanion hole by two hydrogen

bonds donated by the backbone amide nitrogen of Cys-25 and by the sidechain amide nitrogen of Gln-19.

The structure described in this paper clearly indicates that the reaction of papain with leupeptin under the crystallization conditions described generates a single tetrahedral structure in which the oxygen atom sits within the oxyanion hole (Fig. 3). We have found the same backbone donor groups described by Drenth et al. [5] to be positioned sufficiently close to interact with the 'carbonyl' oxygen atom in the papain–leupeptin complex. This therefore lends support to the interpretation of our structure as a tetrahedral adduct. Frankfater et al. [30] proposed a three-step pathway for the inhibition of papain by an aldehyde inhibitor in which two tetrahedral adducts are generated in succession. In the first adduct the oxygen is in the oxyanion hole, whereas in the second it is not. The structure described here is analogous to the first adduct they describe. It is possible that the high concentration of methanol from which the complex was crystallized may have selected in favour of the orientation of the tetrahedral adduct observed.

REFERENCES

[1] Thompson, R.C. (1977) Methods Enzymol. 46, 220–225.

[2] Umezawa, H. (1982) Annu. Rev. Microbiol. 36, 75–99.

[3] Brocklehurst, K., Willenbrock, F. and Salih, E., in: Hydrolytic Enzymes (A. Neuberger and K. Brocklehurst, Eds.), Elsevier, Amsterdam, 1987, pp. 39–158.

[4] Rich, D.H., in: Proteinase Inhibitors (A. Barrett, and G. Salvesen, Eds.), Elsevier, Amsterdam, 1986, pp. 153–178.

[5] Drenth, J., Kalk, K.H. and Swen, H.M. (1976) Biochemistry 15, 3731–3738.

[6] Varughese, K.I., Ahmed, F.R., Carey, P.R., Hasnain, S., Huber, C.P. and Storer, A.C. (1989) Biochemistry 28, 1330–1332.

[7] Yamamoto, D., Matsumoto, K., Ohishi, H., Ishida, T., Inoue, M., Kitamura, K. and Mizuno, H. (1991) J. Biol. Chem. 266, 14771–14777.

[8] Kim, M., Yamamoto, D., Matsumoto, K., Inoue, M., Ishida, T., Mizuno, H., Sumiya, S. and Kitamura, K. (1992) Biochem. J. 287, 797–803.

[9] Aoyagi, T. and Umezawa, H., in: Proteases and Biological Control (E. Reich, D.B. Rifkin and E. Shaw, Eds), Cold Spring Harbor Laboratory, 1975, pp. 429–454.

[10] Ostrowski, L.E., Ahsan, A., Suthar, B., Pagast, P., Bain, D., Wong, C., Patel, A. and Schultz, R. M. (1986) Cancer Res. 46, 4121–4128.

[11] Neblock, D. and Berg, R. (1984) Arch. Biochem. Biophys. 233, 338–344.

[12] Sher, J., Stracher, A., Shafiq, S.A. and Hardy-Stachin, J. (1981) Proc. Natl. Acad. Sci. USA 78, 7742–7744.

[13] Schultz, R., Varma-Nelson, P., Ortiz, R., Kozlowski, K.,

[14] Sluyterman, L. and Wijdenes, J. (1970) Biochim. Biophys. Acta 200, 593–595.

[15] Crawford, C. (1987) Biochem. J. 248, 589–594.

[16] Kamphuis, I.G., Kalk, K.H., Swarte, M.B.A. and Drenth, J. (1984) J. Mol. Biol. 179, 233–256.

[17] Brunger, A., Kuriyan, J. and Karplus, M. (1987) Science 235, 458–460.

[18] Jones, T.A. (1985) Methods Enzymol. 115, 157–171.

[19] Mackenzie, N.E., Grant, S.K., Scott, A.I. and Malthouse, J.P.G. (1986) Biochemistry 25, 2293–2298.

[20] Schecter, I. and Berger, A. (1967) Biochem. Biophys. Res Commun. 27, 157–162.

[21] Stubbs, M.T., Laber, B., Bode, W., Huber, R., Jerala, R., Lenarcic, B. and Turk, V. (1990) EMBO J. 9, 1939–1947.

[22] Menard, R., Carriere, J., Laflamme, P., Plouffe, C., Khouri, H.E., Vernet, T., Tessier, D.C., Thomas, D.Y. and Storer, A.C. (1991) Biochemistry 30, 8924–8928.

[23] Angelides, K.J. and Fink, A.L. (1979) Biochemistry 18, 2355–2363.

[24] Angelides, K.J. and Fink, A.L. (1979) Biochemistry 18, 2363–2369.

[25] Bendall, M.R., Cartwright, I.L., Clark, P.I., Lowe, G. and Nurse, D. (1977) Eur. J. Biochem. 79, 201–209.

[26] Lewis, C.A. and Wolfenden, R. (1977) Biochemistry 16, 4890–4895.

[27] Polgar, L. and Halasz, P. (1982) Biochem. J. 207, 1–10.

[28] Asboth, B. and Polgar, L. (1983) Biochemistry 22, 117–122.

[29] Asboth, B., Stokum, E., Khan, I.U. and Polgar, L. (1985) Biochemistry 24, 606–609.

[30] Frankfater, A. and Kuppy, T. (1981) Biochemistry 20, 5517–5524.

Orawski, A., Pagast, P. and Frankfater, A. (1989) J. Biol. Chem. 264, 1497–1507.